


RESEARCH

Open Access



Secure image transmission through LTE wireless communications systems

Farouk Abduh Kamil Al-Fahaidy^{2,4*} , Radwan AL-Bouthigy³, Mohammad Yahya H. Al-Shamri^{1,2} and Safwan Abdulkareem³

*Correspondence:
farouqakh@gmail.com

¹ Computer Engineering
Department, College
of Computer Science, King Khalid
University, Abha, Saudi Arabia

² Electrical Engineering
Department, Faculty
of Engineering, Ibb University,
Ibb, Yemen

³ Electrical Engineering
Department, Faculty
of Engineering, Sana'a University,
Sana'a, Yemen

⁴ Mechatronics Engineering
Department, Faculty
of Engineering and IT, Emirate
International University-Yemen,
Sana'a, Yemen

Abstract

Secure transmission of images over wireless communications systems can be done using RSA, the most known and efficient cryptographic algorithm, and OFDMA, the most preferred signal processing choice in wireless communications. This paper aims to investigate the performance of OFDMA system for wireless transmission of RSA-based encrypted images. In fact, the performance of OFDMA systems; based on different signal processing techniques, such as, discrete sine transforms (DST) and discrete cosine transforms (DCT), as well as the conventional discrete Fourier transforms (DFT) are tested for wireless transmission of gray-scale images with/without RSA encryption. The progress of transmitting the image is carried by firstly, encrypting the image with RSA algorithm. Then, the encrypted image is modulated with DFT-based, DCT-based, and DST-based OFDMA systems. After that, the modulated images are transmitted over a wireless multipath fading channel. The reverse operations will be carried at the receiver, in addition to the frequency domain equalization to overcome the channel effect. Exhaustive numbers of scenarios are performed for study and investigation of the performance of the different OFDMA systems in terms of PSNR and MSE, with different subcarriers mapping and modulation techniques, is done. Results indicate that the ability of different OFDMA systems for wireless secure transmission of images. However, the DCT-OFDMA system showed superiority over the DST-OFDMA and the conventional DFT-OFDMA systems.

Keywords: Cryptography, DFT, DCT, DST, OFDMA, RSA, Secure wireless image transmission

1 Introduction

Orthogonal frequency division multiple access (OFDMA) is a well-known wireless communication technique which has attracted massive research consideration in industry and academic circles. OFDMA becomes part of new the evolving standards for broadband wireless admittance and was adopted by third-generation partnerships project long-term evaluation (3GPP LTE) as a downlink scheme in WiMAX [1, 2]. In OFDMA systems, the orthogonality among subcarriers is an intrinsic anticipation counter to multiple access interference (MAI). OFDMA can compensate for channel distortions in the frequency domain better than a time-domain equalizer, which requires significant

high computational cost. Recently, several OFDMA systems have been implemented for wireless transmission using Discrete Cosine Transform (DCT), Discrete Sine Transform (DST), and Discrete Wavelet Transform (DWT) [3–6]. However, the OFDMA system suffers from the high peak-to-average power ratio (PAPR) and Carrier Frequency Offsets (CFOs). Many efforts have been made to propose variant OFDMA schemes to improve PAPR, such as DST and DCT compared to the conventional Discrete Fourier Transform (DFT) system. In addition, many PAPR mitigation techniques and CFOs estimation methods are presented [5, 7–16].

Today, the security of the data transmitted in different forms, such as text, images, sounds and videos, is of great importance to most organizations, applications and individuals such as business, social applications; and healthcare. As a result of the growth of the Internet, wireless transmission of plain or secure images and/or video can be easily accomplished over multipath channels; using different wireless communication techniques, such as OFDM, OFDMA; and single-carrier OFDMA systems. Therefore, the performance of OFDMA and SC-FDMA systems for wireless transmission of an image or a compressed image has been studied in many research literature [17–20].

Rivest–Shamir–Adleman (RSA) is the most widely used encryption/decryption algorithm, which is asymmetric prime numbers factorizing technique [21]. RSA is used to encrypt a message and/or the generation of the signature digit of a message. The use of RSA stems from its strongest encryption capability against hacking using a wide variety of large prime numbers.

The RSA algorithm uses two keys, private and public, for the encryption/decryption processes. The public key is shared while the decryption process is kept secret.

The focus of this study is to investigate the performance of different OFDMA systems; introduced for wireless communications recently. In fact, the paper explores the transmission of encrypted images using the RSA algorithm, a well-known public cryptographic algorithm [21]; with different subcarrier mapping methods, Lena image, and different modulation schemes. The main contributions of this paper can be summarized as follows:

- DFT-OFDMA, DCT-OFDMA, and DST-OFDMA systems are employed for the wireless transmission of images with and/or without encryption.
- RSA algorithm is used for encrypting/decrypting the transmitted/received images.
- The performance of DFT-OFDMA, DCT-OFDMA, and DST-OFDMA systems in terms of PSNR and MSE are studied, tested, and investigated.
- The effect of different modulation techniques, QPSK, 16-QAM, and different subcarrier mapping methods, interleaved and localized, are studied and investigated along with different OFDMA systems.

The rest of this paper is organized as follows: Sect. 2 provides an overview of the conventional OFDMA system. Section 3 presents relevant research in the area of wireless secure/insecure image transmission, while Sect. 4 introduces the research methodology and the implemented systems along with their mathematical models for wireless transmission of encrypted images using different recently proposed OFDMA systems.

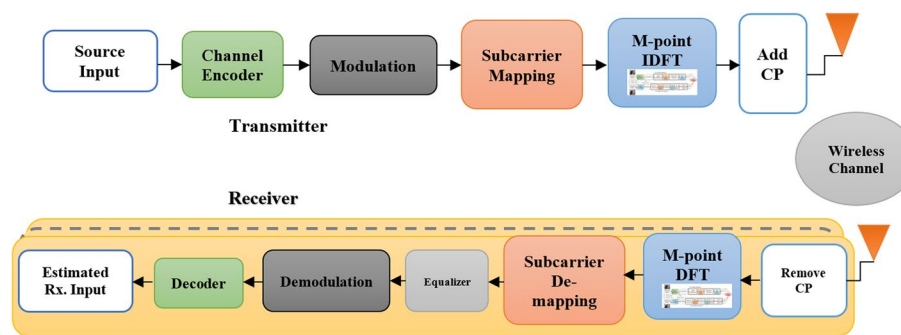


Fig. 1 Conventional OFDMA system model

Section 5 explores the performance of the proposed wireless secure image transmission systems.

2 Conventional DFT-based OFDMA system

OFDMA is a well-known and commonly used wireless communications transmission system that is adopted as a link carrier system in 3GPP LTE and other wireless communication systems [1, 2]. This is due to its several advantages such as efficient utilization of the spectrum using overlapped orthogonal carriers rather than orthogonal bands, immunity to user’s interference, and its support of multiple simultaneous accessing of users [2].

A block diagram of the conventional OFDMA system is shown in Fig. 1. There are Q users with a total of M subcarriers in which each user is randomly assigned to M/Q or N subcarriers. At the transmitter side, the input signal is encoded with a channel coding method, then the signal is modulated using one of the well-known modulation techniques such as; Quadrature Phase Shift Keying (QPSK) or any n -Quadrature Amplitude Modulation (n -QAM). After that, the modulated signals are passed through the OFDMA modulation, by distributing the modulated symbols to the user’s assigned subcarriers using either localized or random (interleaved) mapping methods. After that, the inverse DFT is performed. Finally, before amplifying and transmitting the signal, a small chunk of cyclic prefix (CP), is added for each user to avoid inter-block interference. The resulting signal is wirelessly transmitted over a multipath channel.

At the receiver side, similar operations are carried out in reverse order. Firstly, the CP bits are removed from the received signal. Then, the effect of the multipath channel is avoided in the frequency domain using one of the equalization techniques like, the minimum mean square error (MMSE) equalizer. After that, the resulting signals are passed through the inverse DFT, followed by subcarrier remapping and symbols demodulation. Finally, the demodulated signals are decoded; and the estimated signal is obtained.

3 Related work

There are several attempts to investigate the performance of different wireless transceiver schemes in wireless transmission of images like in [17–19]. In [17], the performance of DFT, DCT and DST-based OFDMA systems for transmitting an unencrypted image was investigated. The presented results showed that OFDMA-based

systems can transmit unencrypted images. The authors of Al-soufy [18] investigated transmission of unsecured images over Single-Carrier Frequency Division Multiple Access (SC-FDMA) system, and the presented results demonstrated this ability. In [19], authors showed the possibility of transmitting unsecured images over DST-based Multi-Carrier Code Division Multiple Access (MC-CDMA) system. In [20], the authors investigated the performance of wireless transmissions of compressed image over DFT-OFDMA, in terms of mean square error (MSE) and peak signal-to-noise ratio (PSNR) metrics. In the area of image data encryption, many research ideas have been proposed for wireless transmission of encrypted images using different encryption techniques such as chaotic, data encryption standard (DES), advanced encryption standard (AES), RSA, and multiple methods [22, 26–32]. Moreover, several attempts have worked on different encryption algorithms to improve the performance of RSA algorithm in terms of execution time [22–25]. Most of these researches are concerned with the transmission of secured images over an Additive-White-Gaussian-Noise (AWGN) channel using Binary Phase Shift Keying (BPSK) modulation technique over different network formations such as computer networks, and/or some traditional/asymmetric encryption methods.

The reported results demonstrated the facility and efficiency of the different OFDMA systems for wireless transmitting of images and the effectiveness of the usage of RSA algorithm for image encryption. So far, there is almost no research that addresses and examines the effectiveness of the OFDMA system in wireless transmitting of encrypted images. Therefore, this led us to study and investigate the wireless transmission of encrypted image using different transceiver schemes of OFDMA based on DFT, DCT, and DST signals carriers.

4 Research methodology

In this section, proposed and implemented system models for wireless transmission of encrypted images are introduced; and their mathematical models are presented.

4.1 Suggested OFDMA mathematical models

Figures 2 and 3 illustrate proposed system models for wireless transmission of encrypted images. These models are based on OFDMA system model with different carrier signal generations techniques, DFT, DCT, or DST. According to the

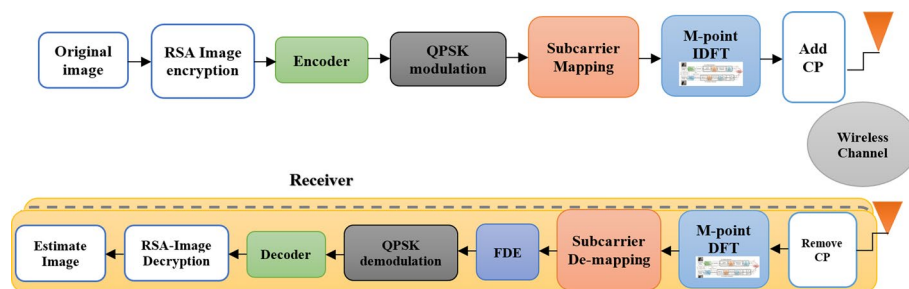


Fig. 2 DFT-based OFDMA system model for encrypted image transmissions over wireless channel

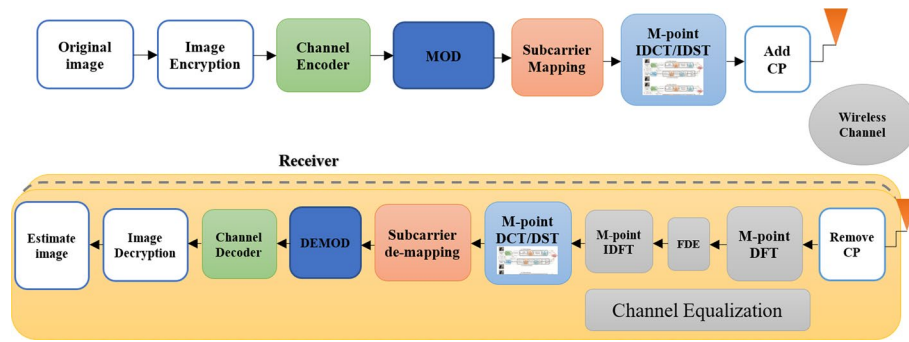


Fig. 3 DCT/DST-based OFDMA system model for encrypted image transmissions over wireless channel

transmitter block diagram, the input signal is an image, which is firstly encrypted using RSA algorithm. The input image, IM , is a gray-scale image results from the conversion of a JPEG image.

The input gray image, IM , of size $R \times C$ can be represented as follows:

$$IM = \begin{bmatrix} Pic_{1 \times 1} & \cdots & Pic_{1 \times C} \\ \vdots & \ddots & \vdots \\ Pic_{R \times 1} & \cdots & Pic_{R \times C} \end{bmatrix}, \tag{1}$$

where the $Pic_{R \times C}$, represent the pixel intensity at row index, R , and column index, C . Then, the 2D matrix is flattened to a 1D vector of length, $L = R \times C$.

$$IV = [val_1, val_2, \dots, val_L]. \tag{2}$$

Hence, the vector, IV , is passed through the RSA encryption process, along with the approved public key, p , and the private encryption key, e . The process of RSA encryption can be represented by the following equation:

$$IV_{enc} = RSA(IV, p, e), \tag{3}$$

such that, the resulted vector, IV_{enc} , can be written as follows:

$$IV_{enc} = [encVal_1, \dots, encVal_L]. \tag{4}$$

Subsequently, the decimal values of the encrypted vector, IV_{enc} , with length, L , is converted to a binary sequence vector, IV_{bin} , of length $8L$. After that, a block of 64-bit size is created for encrypted binary representation of the image. This converts the vector, IV_{bin} , to a 2D binary matrix, $V2$, of size 64-rows and $8L/64$ -columns. There is a possibility to add some extra bits for suitable manipulating of matrix dimensions. These extra bits are added to the last block, and they are removed by the receiver. The resulted 2D matrix, $V2$, is represented as follows:

$$V2 = [BK_1; BK_2; \dots; BK_{CB}], \tag{5}$$

where $CB = 8L/64$, is the number of blocks (columns), and the $BK_1, BK_2, \dots, BK_{CB}$, are the blocks that go through channel encoding, and then they are modulated and transmitted with size 64-bit of a single column each. $V2$ is processed and transmitted block by block and the processing of each block is carried as follows: firstly, a block is encoded

with the Viterbi encoding using trellis convolutional code with a rate equal to 1/2. Then, a modulation technique is applied to the encoded block under the process of transmission. In this work, the QPSK and the 16-QAM modulation techniques are used.

The following step is the OFDMA modulation, which is passed through the subcarriers mapping using, localized and interleaved mapping techniques, and one orthogonal subcarriers generation technique, IDFT, IDST, or IDCT based on the type of OFDMA transceiver scheme that is under working. Assume the input block of a user, i , to the OFDMA modulation is called, B^i . The resulting block/vector after applying the mapping matrix, Ψ^i , of M -rows and N -columns subcarriers for a user, i , is the frequency-domain signal vector, T^i , given by:

$$T^i = \Psi^i B^i. \tag{6}$$

It should be noted that there are only N elements for each user in, T , which are non-zero elements.

After that, an M -point IDFT (t_{DFT}^i), M -point IDCT (t_{DCT}^i), or IDST (t_{DST}^i) is applied to the transform, T , to its time-domain signal, t , which represents the transmitted signal before CP is appended.

$$t_{\text{DFT}}^i = F_M^{-1} T^i = F_M^{-1} \Psi^i B^i, \tag{7}$$

$$t_{\text{DCT}}^i = C_M^{-1} T^i = C_M^{-1} \Psi^i B^i, \tag{8}$$

$$t_{\text{DST}}^i = S_M^{-1} T^i = S_M^{-1} \Psi^i B^i, \tag{9}$$

where F_M^{-1} is the M -point IDFT matrix, C_M^{-1} is the M -point IDCT matrix, and S_M^{-1} is the M -point IDST matrix. Let us in general, name t_{DFT}^i , t_{DCT}^i , and t_{DST}^i as t^i , where t^i is the resulted signal after applying one of inverse Fourier transformers to the modulated signal in Eqs. (7–9).

The last step to be carried by the transmitter is the cyclic prefix (CP) at the beginning of each block serving as a guard band between blocks, such that the inter-block interference is prevented.

At the receiver, after passing of the transmitted signal over the channel and removing the CP, one can write the received signal, r , as:

$$r = \sum_{i=1}^K H_C^i t^i + n, \tag{10}$$

where H_C^i denotes the $M \times M$ circulant channel matrix of the user i , K is the total numbers of users, and n is AWGN vector. The circulant matrix H_C^i can be diagonalized using DFT and IDFT. The H_C^i is expressed as follows:

$$H_C^i = F^{-1} \Lambda^i F, \tag{11}$$

where Λ^i is an $M \times M$ diagonal matrix containing DFT of the circulant sequence of H_C^i . The frequency domain representation of the received signal, R , which is required for frequency domain equalization, can be given by applying DFT to the time-domain received signal, r , as follows:

$$R = F(r). \quad (12)$$

By substituting Eqs. (9) and (11) in Eq. (10) and applying DFT, the received signal, \mathbf{R} , in the frequency domain can be expressed as follows:

$$R = \sum_{i=1}^K \Lambda^i T^i + N, \quad (13)$$

where N is the DFT of the noise n . At this instance, the followed receiver operations, especially, frequency domain equalizer (FDE) and OFDMA demodulation processes are little different, depending on the applied OFDMA subcarriers methods at the transmitter, IDFT, IDCT, or IDST.

4.1.1 DFT-based receiver

In case of DFT-based OFDMA (Fig. 2), the subcarrier de-mapping and FDE operations are carried out and the result is the estimate of the modulated symbols of the i th user:

$$\widehat{B}_N^i = W^i \Psi^{iT} R, \quad (14)$$

where W^i is $N \times N$ FDE matrix of the i th user. Ψ^{iT} is an $N \times M$ matrix of the subcarriers de-mapping of the i th user, which results from the transpose of the subcarrier mapping matrix. FDE equalizer based on the MMSE, W^i , is expressed as in [9]:

$$W_{\text{MMSE}}^i = (\Lambda_d^{iH} \Lambda_d^i + 1/\text{SNR})^{-1} \Lambda_d^{iH}, \quad (15)$$

where Λ_d^i is the frequency domain channel after the de-mapping process is performed.

4.1.2 IDST/IDCT transmitter

For DCT-based or DST-based OFDMA system model illustrated in Fig. 3, the FDE process is carried using MMSE equalizer with, W^i matrix (Eq. (15)) of size $M \times M$ followed by M -point IDFT. The resulted signal from the equalizer for the i th user is written as follows:

$$\widehat{r}^i = \text{IDFT}(W^i R). \quad (16)$$

After that, DCT or DST process is performed and followed by the subcarrier de-mapping. The result is the estimate of the modulated symbols of the i th user:

$$\widehat{B}_N^i = \Psi^{iT} C_M \widehat{r}, \quad (17)$$

$$\widehat{B}_N^i = \Psi^{iT} S_M \widehat{r}, \quad (18)$$

where C_M and S_M are DCT; and DST transforms, respectively. The next step is the demodulation process of the resulted block of symbols for generating the corresponding demodulated bits. Subsequently, the channel decoding is performed using trellis decoding technique. This process is repeated for all constituted blocks of the transmitted image. All received blocks are arranged and the extra bits that are added to the last sent block are removed.

By arranging the received binary blocks, a binary vector of size $64CB$ bits corresponds to the received encrypted image is formed. This binary vector is converted to a decimal vector, where each decimal value is a representation of an 8-bit gray value. The resultant vector is a vector of size $64CB/8$. This vector is reshaped to a 2D matrix of 256×256 rows and columns, like the encrypted vector, IVh_{enc} . The vector, IVh_{enc} , represents the received estimated vector of the sent encrypted and reshaped image, that can be represented as:

$$IVh_{enc} = [encIValh_1, \dots, encValh_{TT}]. \tag{19}$$

Then, the encrypted vector, IVh_{enc} , is passed through the RSA decryption algorithm along with the private decryption key, d , where $d = inv(e)$, and the public key, p . The process of decrypting the received encrypted image which results with estimated received image, IVh , can be modeled as follows:

$$IVh = [RSA_{dec}(IVh_{enc}, p, d)]. \tag{20}$$

The estimated and decrypted image is reshaped again to a matrix, IMh , of 256×256 pixels and expressed as follows:

$$IMh = \begin{bmatrix} Pic_{1 \times 1} & \cdots & Pic_{1 \times C} \\ \vdots & \ddots & \vdots \\ Pic_{R \times 1} & \cdots & Pic_{R \times C} \end{bmatrix}. \tag{21}$$

Finally, the estimated received image, IMh , is compared with the transmitted image in the gray-scale form of the transmitted image.

4.2 Study of the computational complexity

The computation complexity of the proposed wireless image transmission system models, DFT-OFDM, DST-OFDMA, and DCT-OFDMA, was studied and compared. Table 1 illustrates the complexity of the transmitters with IDST and IDCT. There is a slight improvement due to the use of either sine or cosine orthogonal subcarriers

Table 1 Comparative study of the computation complexity of DFT-based, DCT-based, and DST-based OFDMA models

OFDMA model	Transmitter/receiver	Computations
DFT-based	Tx	$M \times M$ Multiplications and $M \times M$ Additions
	Rx	$M \times M$ Multiplications and $M \times M$ Additions Equalizer with N-point No IDFT is applied
DCT-based	Tx	$M \times M$ Multiplications only
	Rx	$M \times M$ DFT Multiplications and $M \times M$ DFT Additions Equalizer with M-point M-point IDFT is applied, M-point DCT is followed
DST-based	Tx	$M \times M$ Multiplications only
	Rx	$M \times M$ DFT Multiplications and $M \times M$ DFT Additions Equalizer with M-point M-point IDFT is applied, M-point DST is followed

signal processing technique, as compared to the conventional DFT-based OFDMA system, which uses a complex form of cosines and sines for providing of the orthogonal subcarriers. At the receiver, the computation complexity of the DST-based and the DCT-based OFDMA systems are slightly higher compared to the conventional DFT-based system. This is due to the need of the DFT/IFFT blocks for channel equalization in DST-based and DCT-based receivers. Nevertheless, this slight increase in the computation complexity of the receiver, may be not so important, especially in uplink transmission, where the receiver is the base station.

5 Simulation, experiments and discussion

This section gives a simulation of the conducted experiments and then discusses the results of the proposed systems: DFT-IOFDMA, DFT-LOFDMA, DST-IOFDMA, DST-LOFDMA, DCT-IOFDMA, and DCT-LOFDMA, where *I* refers to interleaved, and *L* for localized subcarriers mapping. These different models of the OFDMA with localized and interleaved subcarriers mapping methods based on DFT, DCT and DST are employed and investigated for wireless transmissions of encrypted images.

The experiments of different OFDMA systems for transmission of Lena image (Fig. 4a) with two modulation techniques, QPSK and 16-QAM, are carried out using MATLAB-2016 Software environment on a DELL computer, Core-i3 with RAM of 4 GB. A Monte Carlo simulation is used for all simulation scenarios that are: 108,480 scenarios for QPSK modulation, $2(\text{images}) \times \text{number of blocks (9040 for QPSK and 2048 for 16-QAM)} \times 2(\text{mapping methods}) \times 3(\text{different OFDMA systems})$, and 24,576 scenarios for 16-QAM modulation. This results in a total of 133,056 scenarios. In addition, investigation experiments are carried for the DCT-OFDMA with cameraman image shown in Fig. 4b.

These simulation scenarios play as a good indication to different vendors for demonstrating the tradeoffs between different effective configuration key parameters that are considered in the establishment of the wireless transmission systems of the encrypted images.



a: Lena Image



b: Cameraman Image

Fig. 4 **a** Lena image, **b** cameraman image

Table 2 Simulation configuration parameters

	Parameter	Value(s)
Transmitter	Simulation method	Monte Carlo
	Input images	Lena images
	Block size	64 bits
	Channel coding	Trellis convolutional code, rate 1/2
	No. of users	4
	Total number of carriers (DFT/DCT/DST Size)	256 bits
	Encryption algorithm	RSA encryption
	Modulation techniques	QPSK and 16-QAM
	Carrier mapping techniques	Localized and interleaved
	Cyclic prefix	20 samples
Channel	System bandwidth	5 MHz
	Channel model	Vehicular A. Channel
	Noise	AWGN
	Channel estimation	Perfect
Receiver	Equalization	MMSE
	Decryption algorithm	RSA Decryption
Ranges of SNR	SNR (dB)	0, 5,10, 15, 20, 25,30, 35

5.1 Simulation configuration parameters and performance measure metrics

Table 2 presents and shows the configuration parameters used and their corresponding values. The proposed systems performance in terms of MSE and PSNR are investigated to study the effectiveness of each of the proposed system model with respect to different signal-to-noise ratio (SNR) values. The MSE is expressed as:

$$MSE = \frac{\sum_{i=1}^N \sum_{j=1}^N (Im_T(i,j) - Im_R(i,j))^2}{N^2}, \tag{22}$$

where N is the number of rows/columns pixels, and Im_T and Im_R are the transmitted and the received images, respectively. PSNR defines the ratio between the maximum probable power of a signal to the demeaning noise power that disrupts the dependability of the signal. It is expressed as follows:

$$PSNR = 10\log_{10} \left(\frac{Pic_{max}^2}{MSE^2} \right), \tag{23}$$

where Pic_{max} is the maximum value of image’s pixels which is assumed 255 in case of gray-scale image and therefore, the previous equation can be rewritten as follows:

$$PSNR = 10\log_{10} \left(\frac{255^2}{MSE^2} \right). \tag{24}$$

5.2 Performance study and investigations

This subsection examines the performance of the proposed systems in terms of MSE and PSNR of the received image, with/without encryption. These results provide a good indication of the effect of the encryption process on the performance of the proposed

Table 5 PSNR values of the received image without RSA encryption, using 16-QAM modulation and different subcarriers mapping methods

SNR [dB]	DFT-OFDMA		DCT-OFDMA		DST-OFDMA	
	DFT-LOFDMA	DFT-IOFDMA	DCT-LOFDMA	DCT-IOFDMA	DST-LOFDMA	DST-IOFDMA
0	28.2883	28.2349	29.4765	29.1328	28.2367	28.2575
5	28.3601	28.1634	30.2378	29.4022	28.3004	28.1114
10	29.4397	29.0117	32.2950	32.1861	29.2597	28.8732
15	32.2672	32.8441	37.4806	39.6453	31.6865	32.0007
20	37.4269	41.1872	46.0558	49.4004	37.2600	39.3936
25	43.7650	51.4515	58.1279	Inf.	44.9389	49.2409
30	51.9278	Inf.	Inf.	Inf.	56.1740	61.2700
35	Inf.	Inf.	Inf.	Inf.	Inf.	Inf.

Table 6 PSNR values of the received image with RSA encryption, using 16-QAM modulation and different subcarriers mapping methods

SNR [dB]	DFT OFDMA		DCT OFDMA		DST OFDMA	
	DFT-LOFDMA	DFT-IOFDMA	DCT-LOFDMA	DCT-IOFDMA	DST-LOFDMA	DST-IOFDMA
0	28.5279	28.5483	28.6475	28.6184	28.4977	28.4929
5	28.5138	28.4685	28.8915	28.7422	28.5107	28.4756
10	29.0148	28.7591	30.7821	30.9158	28.8321	28.7049
15	31.4021	31.7790	35.7290	38.1194	30.6131	30.9957
20	36.3356	39.7319	42.9669	48.1801	35.6885	38.2799
25	43.1750	49.6354	53.7800	55.8987	42.8036	48.0213
30	51.6638	58.9412	65.8777	64.1737	53.1565	59.7577
35	61.0908	Inf.	Inf.	Inf.	60.2136	Inf.

transmission of Lena image without encryption. For example, at SNR = 20 dB, the values of the PSNR of DFT-LOFDMA and DFT-IOFDMA of the received unencrypted Lena image are 48.9089 and 54.3937, respectively. The corresponding PSNR values of the received decrypted image are 46.9117 and 54.1237. They showed slightly low differences of PSNR values, especially with interleaved mapping. Likewise, for DST-based OFDMA system with localized and interleaved mapping and at SNR = 20 dB, PSNR differences are bit small. Obviously, DCT-LOFDMA and DCT-IOFDMA systems are given the same, an infinite value of PSNR, in all cases. The results demonstrated an acceptable degradation of PSNR of the received decrypted image, especially in case of DCT-based OFDMA system. Moreover, DCT and DST-based OFDMA systems provide better results of PSNR in transmission of encrypted image, in comparison with DFT OFDMA used for transmitting image without encryption. Take as a comparison example the value of PSNR for any value of SNR from 0 to 20 dB, for DCT-OFDMA and DST-OFDMA systems, respectively.

Similarly, Tables 5 and 6 show the experimental results in term of PSNR versus SNR, for 16-QAM modulation without and with RSA encrypting of Lena image, respectively. The results showed the effectiveness of DFT-based, DCT-based, and DST-based OFDMA systems for wireless transmission of unencrypted/encrypted

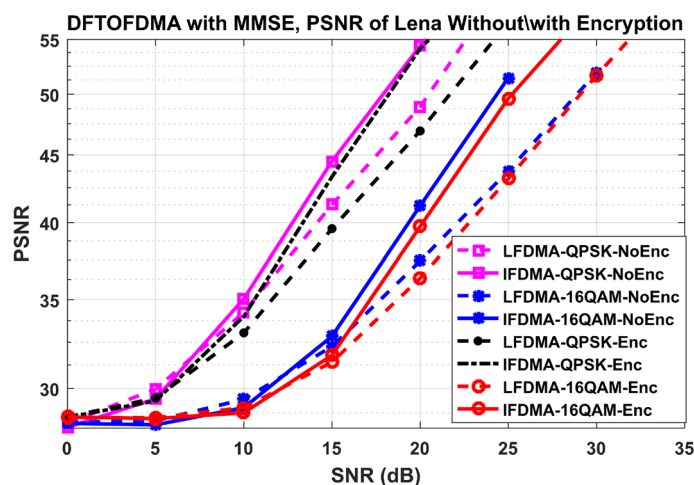


Fig. 5 PSNR versus SNR of the Lena image with/without RSA encryption over DFT-OFDMA

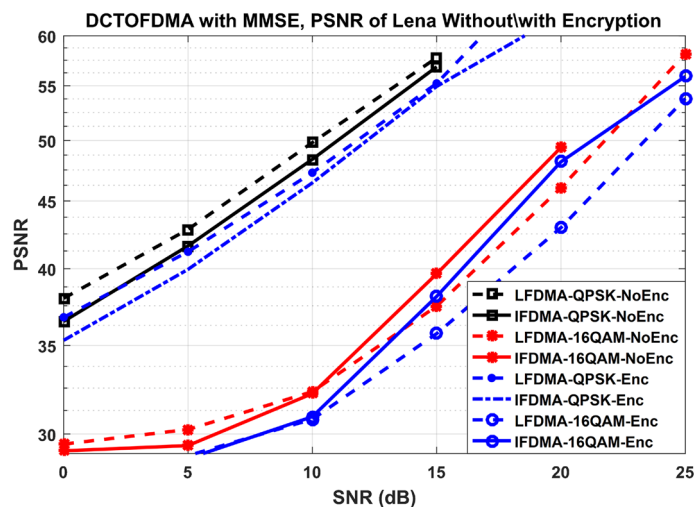


Fig. 6 PSNR versus SNR of the Lena image with/without RSA encryption over DCT-OFDMA

images. As SNR values increases, PSNR values increased. The DCT-based OFDMA system with 16-QAM modulation reveals the best performance, in terms of PSNR, as compared with DFT- and DST-based OFDMA systems. Moreover, PSNR difference of the received decrypted image and the received unencrypted image is slightly low but it is acceptable. Regarding the subcarrier mapping methods, the interleaved mapping of subcarriers reveals a better performance when compared to the localized mapping in most scenarios. As a conclusion, OFDMA system has approved its suitability for the transmission of either the unencrypted images and/or the encrypted images. Unambiguously, DCT-based OFDMA system showed its performance as a promising wireless transmission system of secured/encrypted images.

For further investigation, the PSNR versus SNR relationship curves are given for different scenarios in Figs. 5, 6 and 7. Figure 5 depicts PSNR versus SNR curves of DFT-based OFDMA wireless transmission system, when it is used for transmitting Lena and

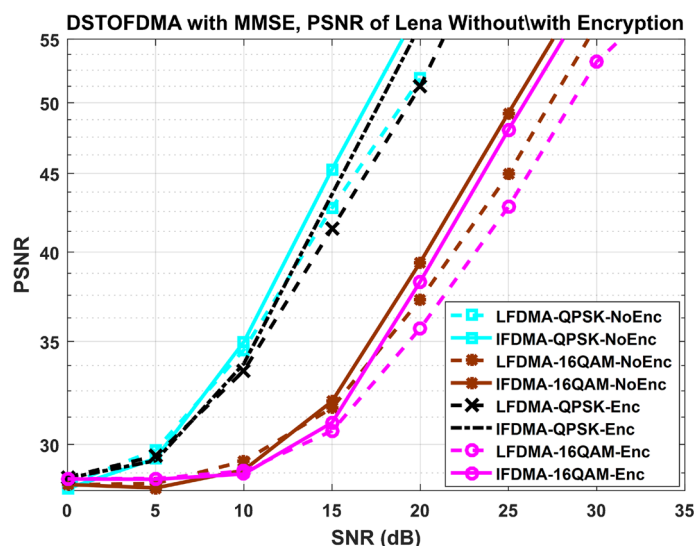


Fig. 7 PSNR versus SNR of the Lena image with/without RSA encryption over DST-OFDMA

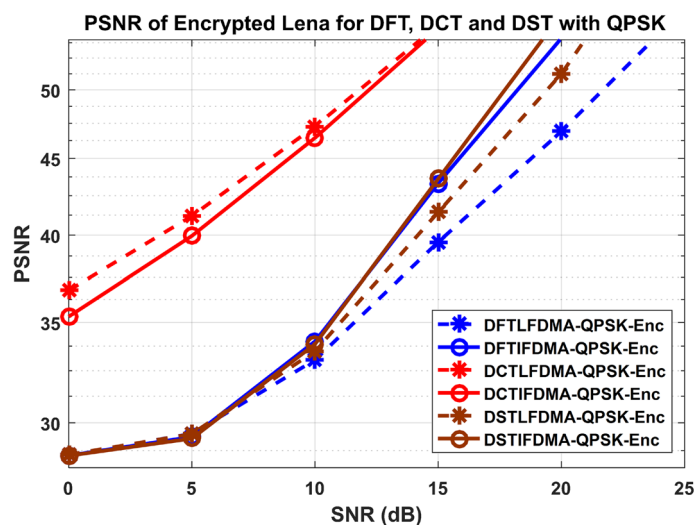


Fig. 8 A comparison of PSNR versus SNR of the received encrypted Lena image using DFT, DCT and DST OFDMA

its RSA's encrypted images. These curves show acceptable decreasing of PSNR values of the encrypted Lena image, for the two subcarriers mapping methods, the localized and the interleaved, and QPSK and 16-QAM modulation techniques.

Likewise, Figs. 6 and 7 illustrate PSNR versus SNR curves of DCT and DST-based OFDMA systems when they are used in transmitting encrypted Lena image, as compared to the transmitted unencrypted Lena image. These different curves show the two proposed systems with QPSK and 16-QAM modulation techniques and the localized and interleaved subcarriers mapping. It is observed that the different proposed OFDMA systems are effective for transmitting images with/without encryption. To understand more the performance of the proposed DCT-OFDMA system in terms

of PSNR. Figure 8 demonstrates the proficiency of DCT-OFDMA system compared to other proposed DFT- and DST-based OFDMA systems with QPSK modulation and different subcarriers mapping. Moreover, interleaved mapping has shown a good improvement of the performance in terms of PSNR.

5.2.2 MSE performance

Several experiments were carried out for studying and investigating the performance of the proposed systems, in terms of MSE performance metric, used for wireless transmission of encrypted/unencrypted Lena images.

Tables 7 and 8 are itemized MSE values at different SNR values for the proposed DFT-OFDMA, DCT-OFDMA, and DST-OFDMA systems, used in plain and secure transmissions of Lena image with QPSK modulation and two different subcarriers mapping methods. The three proposed systems showed their efficiency and competence in wireless transmission of plain and/or secure images. The MSE results showed that the MSE decreased as the SNR increased, yet the transmitted image was either a plain image or an encrypted image. Moreover, the differences of MSE between of the received plain and encrypted images are insignificant. However, the proposed

Table 7 MSE values of the received image without RSA encryption, using QPSK modulation and different subcarriers mapping methods

SNR [dB]	DFT-OFDMA		DCT-OFDMA		DST-OFDMA	
	DFT-LOFDMA	DFT-IOFDMA	DCT-LOFDMA	DCT-IOFDMA	DST-LOFDMA	DST-IOFDMA
0	0.1149	0.1300	0.0066	0.0082	0.1160	0.1302
5	0.0648	0.0640	0.0020	0.0024	0.0642	0.0651
10	0.0240	0.0157	4.6777e-04	5.2807e-04	0.0196	0.0151
15	0.0059	0.0016	8.6958e-05	9.1553e-05	0.0033	0.0017
20	0.0012	1.3080e-04	0	0	3.2954e-04	7.0627e-05
25	7.5187e-05	1.2338e-05	0	0	0	0
30	0	0	0	0	0	0
35	0	0	0	0	0	0

Table 8 MSE values of the received image with RSA encryption, using QPSK modulation and different subcarriers mapping methods

SNR [dB]	DFT OFDMA		DCT OFDMA		DST OFDMA	
	DFT-LOFDMA	DFT-IOFDMA	DCT-LOFDMA	DCT-IOFDMA	DST-LOFDMA	DST-IOFDMA
0	0.1251	0.1262	0.0185	0.0264	0.1257	0.1264
5	0.0999	0.1045	0.0061	0.0088	0.1005	0.1058
10	0.0448	0.0348	0.0016	0.0020	0.0395	0.0353
15	0.0095	0.0040	3.2481e-04	2.4414e-04	0.0059	0.0035
20	0.0014	3.7482e-04	1.2136e-05	5.9751e-05	5.9509e-04	1.5259e-04
25	1.3733e-04	4.5776e-05	0	0	1.5259e-05	1.5259e-05
30	0	1.0108e-05	0	0	0	0
35	0	0	0	0	0	0

Table 9 MSE values of the received image without RSA encryption, using 16-QAM modulation and different subcarriers mapping methods

SNR [dB]	DFT-OFDMA		DCT-OFDMA		DST-OFDMA	
	DFT-LOFDMA	DFT-IOFDMA	DCT-LOFDMA	DCT-IOFDMA	DST-LOFDMA	DST-IOFDMA
0	0.1563	0.1611	0.1096	0.1409	0.1601	0.1619
5	0.1092	0.1378	0.0421	0.0688	0.1164	0.1416
10	0.0487	0.0655	0.0146	0.0186	0.0551	0.0705
15	0.0158	0.0169	0.0039	0.0023	0.0183	0.0208
20	0.0032	0.0025	6.1035e-04	1.8311e-04	0.0032	0.0028
25	7.4768e-04	1.5259e-04	3.0518e-05	0	4.4250e-04	1.3733e-04
30	9.1553e-05	0	0	0	9.1125e-05	1.5259e-05
35	0	0	0	0	0	0

Table 10 MSE values of the received image with RSA encryption, using 16-QAM modulation and different subcarriers mapping methods

SNR [dB]	DFT-OFDMA		DCT-OFDMA		DST-OFDMA	
	DFT-LOFDMA	DFT-IOFDMA	DCT-LOFDMA	DCT-IOFDMA	DST-LOFDMA	DST-IOFDMA
0	0.1286	0.1285	0.1257	0.1276	0.1296	0.1284
5	0.1261	0.1273	0.1126	0.1185	0.1251	0.1277
10	0.1108	0.1165	0.0715	0.0686	0.1155	0.1182
15	0.0624	0.0581	0.0205	0.0128	0.0725	0.0688
20	0.0182	0.0092	0.0039	0.0013	0.0218	0.0125
25	0.0037	8.4677e-04	3.5095e-04	1.9034e-04	0.0040	0.0012
30	6.1711e-04	6.1035e-05	1.5259e-05	1.6825e-05	3.8147e-04	6.1035e-05
35	5.0617e-05	0	0	0	4.5776e-05	0

DCT-OFDMA system has approved its effectiveness in wireless transmission of Lena image with or without encryption.

In the same way, Tables 9 and 10 are documented MSE values at different SNR values for the proposed systems when they are used in plain and secure transmissions of Lena image with 16-QAM modulation and the localized and interleaved subcarriers mapping methods. Likewise, the proposed systems have verified their capabilities and DCT-OFDMA is again the winner, with the top performance in terms of MSE metric. Intuitively, this is what was expected from the proposed DCT-OFDMA system, due to the energy compaction property of DCT. The energy compaction property of DCT gives DCT-OFDMA system the ability to exploit the channel diversity, and therefore, to compact the channel effect [3].

Figures 9, 10 and 11 illustrate the MSE versus SNR of the received encrypted and unencrypted Lena image, when transmitted via DFT-OFDMA, DCT-OFDMA, and DST-OFDMA proposed systems, respectively, with QPSK and 16-QAM modulation techniques and the localized and interleaved subcarriers mapping methods. The curves showed how MSE decreased as SNR increases. There was a small degradation effect in case of the received encrypted image.

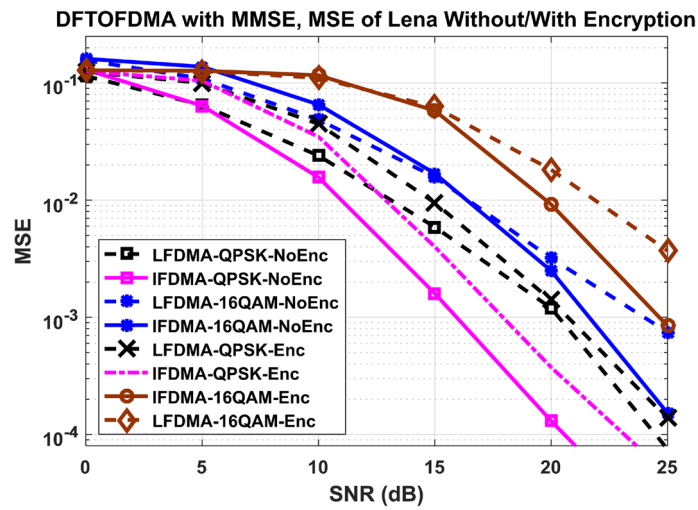


Fig. 9 MSE versus SNR of the Lena image with/without RSA encryption over DFT-OFDMA

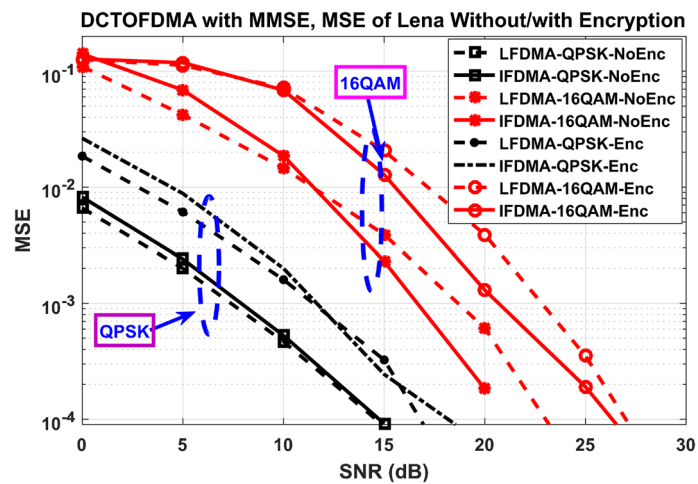


Fig. 10 MSE versus SNR of the Lena image with/without RSA encryption over DCT-OFDMA

Looking at the different modulation, QPSK and 16-QAM results, a logical behavior of performance is perceived with better results for QPSK. Further, the interleaved subcarrier mapping presents better performance in terms of MSE for most scenarios, especially when SNR is increased from 15dB, except in DCT-OFDMA with QPSK modulation, it has little influence. Figure 12 depicts MSE performance for different proposed systems with QPSK modulation, used for transmission of encrypted Lena image. DCT-OFDMA showed itself as the prominent choice in comparison with other proposed systems, DFT-OFDMA and DST-OFDMA. In synopsis, DCT-OFDMA system with interleaved mapping has the better performance in transmission of encrypted image using RSA encryption algorithm.

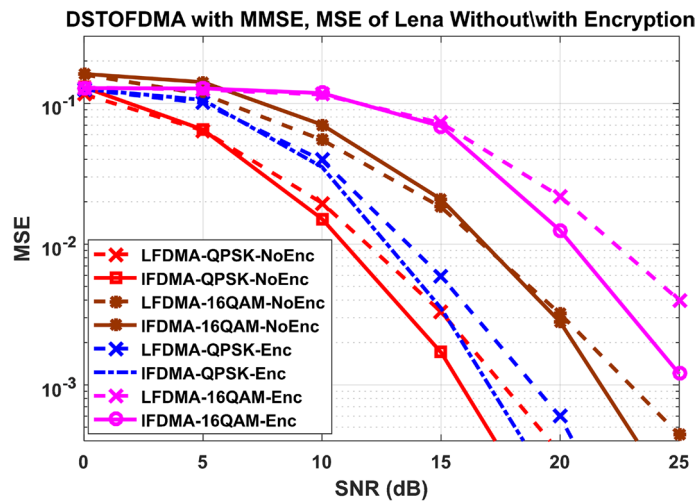


Fig. 11 MSE versus SNR of the Lena image with/without RSA encryption over DST-OFDMA

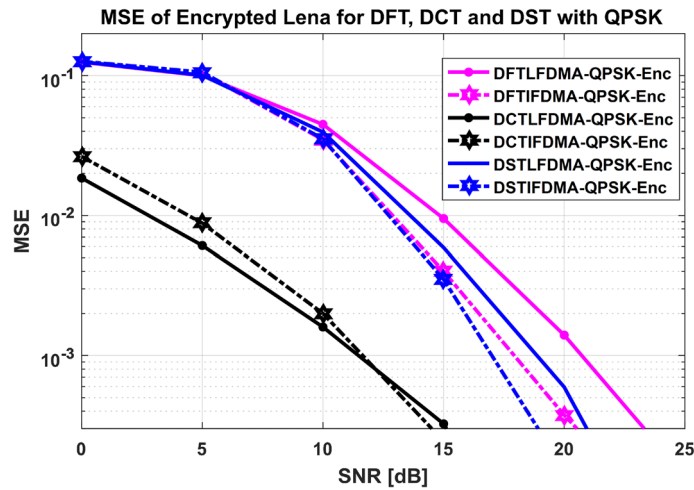


Fig. 12 A comparison of MSE versus SNR of the received encrypted Lena image using DFT, DCT and DST OFDMA

5.2.3 A clarity investigation of the received images

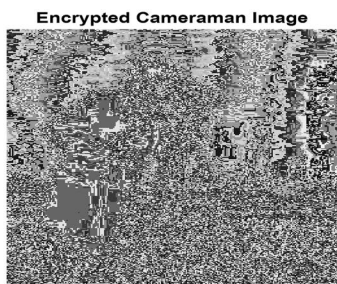
Figure 13a, b and c shows visually the quality of the reconstructed images, after the encrypted original image was transmitted using DFT-OFDMA, DCT-OFDMA, and DST-OFDMA systems with QPSK modulation and interleaved mapping, when SNR is equal to 15dB. In comparison with the original Lena image shown in Fig. 4, we can conclude the superiority of DCT-OFDMA system over DCT-OFDMA and DFT-OFDMA systems.

5.3 Investigation of the proposed systems with cameraman image

This subsection investigates and approves the performance of the proposed systems using another image, the cameraman image, shown in Fig. 4b. The performance of the proposed systems, the DCT-LOFDMA and the DCT-IOFDMA systems has been

Table 12 MSE vs. SNR of the received cameraman image with/without RSA encryption

SNR [dB]	DCT OFDMA without RSA encryption, QPSK		DCT OFDMA with RSA encryption, QPSK		DCT OFDMA without RSA encryption, 16QAM		DCT OFDMA with RSA encryption, 16QAM	
	DCT-LOFDMA	DCT-IOFDMA	DCT-LOFDMA	DCT-IOFDMA	DCT-LOFDMA	DCT-IOFDMA	DCT-LOFDMA	DCT-IOFDMA
20	0	9.1717e-06	8.0623e-04	8.2945e-04	9.7656e-04	3.5095e-04	0.0041	0.0023
25	0	0	0	8.1371e-04	1.5259e-05	3.0518e-05	0.0012	0.0010
30	0	0	0	0	0	0	8.2653e-04	8.1619e-04
35	0	0	0	0	0	0	0	0



(a) The Tx. Encrypted Cameraman Image



(b) The Rx. Image with QPSK, and SNR = 20dB



(c) The Rx. Image with 16QAM, and SNR = 20dB

Fig. 14 Reconstructed cameraman images using DCT-OFDMA with QPSK and 16QAM modulation, at SNR = 20dB

As depicted in previous tables and figures, the performance results in terms of, MSE and PSNR, shown in Tables 11 and 12 have agreed the relevance of the proposed systems for secure wireless transmissions of images. Moreover, the visual appearance of the received/reconstructed images exposed in Fig. 14 has shown and verified a good performance of the proposed system for wireless transmission of encrypted images. Even when different images are used/employed.

5.4 Comparison with literatures

This subsection has presented a brief comparison with literature research related to this work. Table 13 presents a summary comparison of recent researches that are related to our work.

Table 13 A summary comparison with related works

Research	Contribution	Encrypted image or not	Environment (network type)
Ref. [17]	Wireless image transmission of images using OFDMA system	No	OFDMA over Vehicular Channel, with QPSK and 16QAM modulation
Ref. [18]	Performance evaluation of wireless image transmission using SC-FDMA system	No	SC-FDMA over Vehicular Channel, with QPSK and 16QAM modulation
Ref. [19]	New image transmission schemes for DST-based MC-CDMA system	No	DST-based MC-CDMA system
Ref. [22]	Application of data image encryption technology in computer networks	Yes	Computer networks
Ref. [28]	Secure image transmission over wireless network	Yes	Ideal Channel with Turbo code is used as Channel coding, Keys generator and Chaotic Henon map encryption
Our work	Investigation and approval of the capability of OFDMA System in wireless transmission of encrypted image	Yes	OFDMA over Vehicular Channel, with QPSK and 16QAM Modulation, RSA-based image encryption

It is noted from the presented table, that there is no work carried for the examination of secure wireless image transmissions over OFDMA and any other orthogonal-based wireless transmission systems, like in [17–19]. Other works have tested the transmission of encrypted image either, over ideal wireless channels with AWGN using turbo channel coding like in [28], or over computer network like in [22].

The performance comparison of the proposed systems results can be compared with the results in [17]. For example, results in Tables 3 and 5 are compared with results in Tables 4 and 6. It is noted that the proposed systems have an acceptable performance degradation due to the RSA encryption.

6 Conclusions

This research studies and investigates exciting wireless transmission of RSA-based encrypted gray-scale images, using OFDMA systems with different orthogonal basis functions, two different subcarriers mapping methods, and two different modulation techniques. In addition, the proposed systems, DFT-OFDMA, DCT-OFDMA, and DST-OFDMA are compared to their practice in wireless transmission of original image without encryption. In addition, many systems, DFT-OFDMA, DCT-OFDMA, and DST-OFDMA that are implemented and compared for wireless transmission of original image with and without encryption was proposed.

The results showed the capability of the proposed OFDMA systems for transmitting gray-scale images, with/without RSA encryption. This study showed that wireless transmission of RSA-based encrypted images is possible using different orthogonal-carriers basis functions, different images, different subcarrier mapping methods, and different modulation techniques. However, the DCT-OFDMA system showed a significant performance enhancement in terms of PSNR and MSE metrics, when compared to DFT-OFDMA and DST-OFDMA systems for the most performed scenarios.

In respect to the modulation techniques and subcarrier mapping methods, QPSK modulation and the interleaved mapping have shown a significant enhancement of the

performance in terms of PSNR and MSE as compared to 16-QAM modulation and localized mapping for all systems. In the receiving end, DCT-OFDMA system with QPSK modulation has shown the finest clarity of the reconstructed images than DFT-OFDMA and DST-OFDMA systems. Moreover, the interleaved mapping method delivers better performance in terms of PSNR and MSE, than the localized mapping method for all tested systems, especially for PSNR more than or equal to 15dB with QPSK modulation.

Abbreviations

LTE	Long-term evaluation
OFDMA	Orthogonal frequency division multiple access
MAI	Multiple access interference
DCT	Discrete cosine transform
DST	Discrete sine transform
DWT	Discrete wavelet transform
PAPR	Peak-to-average power ratio
CFOs	Carrier frequency offsets
DFT	Discrete Fourier transform
RSA	Rivest–Shamir–Adleman
DFT-OFDMA	Discrete Fourier transform orthogonal frequency division multiple access
DCT-OFDMA	Discrete cosine transform orthogonal frequency division multiple access
DST-OFDMA	Discrete sine transform orthogonal frequency division multiple access
QPSK	Quadrature phase shift keying
n-QAM	N-quadrature amplitude modulation
CP	Cyclic prefix
MMSE	Minimum mean square error
SC-FDMA	Single carrier frequency division multiple access
MC-CDMA	Multi-carrier Code Division Multiple Access
DES	Data Encryption Standard
AES	Advanced Encryption Standard
AWGN	Additive-White-Gaussian-Noise
BPSK	Binary phase shift keying
IM	Input image
FDE	Frequency domain equalizer
MSE	Mean square error
PSNR	Peak signal-to-noise ratio
SNR	Signal-to-noise ratio

Acknowledgements

The authors extend their appreciation to the Deanship of Scientific Research, at King Khaled University for funding this work through Large Group Project under grant number (RGP.2/408/44).

Author contributions

Authors declare that they have no conflict of interest.

Funding

The Deanship of Scientific Research, at King Khaled University, Large Group Project under grant number (RGP.2/408/44).

Availability of data and materials

Data and materials are available upon request.

Declarations

Competing interests

The authors declare that they have no known competing financial interests or personal relationships that could have appeared to influence the work reported in this paper.

Received: 7 April 2023 Accepted: 31 December 2023

Published online: 10 January 2024

References

1. 3rd Generation Partnership Project (3GPP) Technical Specification Group Radio Access Network; Physical Layer Aspects for Evolved Universal Terrestrial Radio Access (UTRA) (Release 7). 3GPP TR 25. 814, V7. 1. 0 (2006)
2. Air Interface for Fixed and Mobile Broadband Wireless Access Systems Amendment for Physical and Medium Access Control Layers for Combined Fixed and Mobile Operation in Licensed Bands, IEEE Std 802. 16e (2006)

3. F.A.K. Al-fuhaidy, H.E.A.K. Hassan, K. El-barbary, A new transceiver scheme for OFDMA system based on discrete cosine transform and phase modulations. *Wirel. Pers. Commun.* **69**, 1735–1748 (2012). <https://doi.org/10.1007/s11277-012-0660-0>
4. F.S. Al-kamali, M.I. Dessouky, B.M. Sallam, F. Shawki, F.E. Abd El-Samie, Transceiver scheme for single-carrier frequency division multiple access implementing the wavelet transform and peak-to-average power ratio reduction methods. *IET Commun.* **4**(1), 69–79 (2010)
5. F.A.K. Al-Fuhaidy, K. Al-sofy, F.S. Alkamali, Discrete sine transform based OFDMA system for wireless broadband communications. *AASCIT Commun.* **6**(1), 13–21 (2019)
6. P.Tan, N.C. Beaulieu, A comparison of DCT-based OFDM and DFT-based OFDM in frequency offset and fading channels. *IEEE Trans. Commun.* **54**(11), 2113–2125 (2006)
7. F.S. Al-Kamali, A new single-carrier transceiver scheme based on the discrete sine transform. *J. Eng.* **2014**(5), 214–218 (2014)
8. J. Armstrong, Peak-to-average power reduction for OFDM by repeated clipping and frequency domain filtering. *Electron. Lett.* **38**, 246–247 (2002)
9. S.-H. Wang, J.-C. Xie, S.-P. Li, A low-complexity SLM PAPR reduction scheme for interleaved OFDMA uplink. *GLOBE-COM Conference*, IEEE Publisher (2009)
10. S.C. Thompson, A.U. Ahmed, J.G. Proakis, J.R. Zeidler, M.J. Geile, Constant envelope OFDM. *IEEE Trans. Commun.* **56**(8), 1300–1312 (2008)
11. H.E.A. Hassan, F.A.K. Al-fuhaidy, Kh. El-barbary, Peak-to-average power ratio reduction for single carrier-frequency division multiple access using repeated clipping and filtering. *ASAT—14th Conf. ASAT-14-219-CM* (2011)
12. S. Zid, R. Bouallegue, Low-complexity PAPR reduction schemes using SLM and PTS approaches for interleaved OFDMA. *International Conference on Ultra Modern Telecommunications & Workshops*, IEEE publisher (2009)
13. F.A.K. Al-Fuhaidy, F.S. Alkamali, K.A. Al-Soufy, DFT-based OFDMA system with phase modulation for broadband communication. *AJECE J.* **3**(1), 1–9 (2019). <https://doi.org/10.11648/j.ajece.20190301.11>
14. H.G. Myung, J. Lim, D.J. Goodman, Peak-to-Average power Ratio of Single Carrier FDMA Signals with Pulse Shaping. *Proceeding of the IEEE PIMRC* (2006)
15. F.A.K. Al-Fuhaidy, F.S. Alkamali, K. Al-sofy, Phase modulated OFDMA system, study and investigations. *Am. J. Comput. Sci. Appl.* (2019)
16. H.E.A. Hassan, F.A.K. Al-fuhaidy, Kh. El-barbary, Peak-to-average power ratio reduction of uplink broadband transmission systems using different reduction algorithms. *ASAT—14th Conf. ASAT-14-220-CM*, May. 24–26 (2011)
17. F.S. Al-kamali, F.A. Al-fuhaidy, K.A. Al-soufy, Wireless image transmissions over frequency selective channel using recent OFDMA systems. *Am. J. Comput. Commun. Control.* **5**(1), 30–38 (2018)
18. K.M. Al-soufy, F.S. Al-kamali, F.A. Al-fuhaidy, Performance evaluation of SC-FDMA systems using wireless images. *Am. J. Comput. Sci. Appl.* **1**, 11 (2017)
19. F.S. Al-Kamali, A.F. Al-Junaid, M.Y. Al-Shamri, New image transmission schemes for DST-based MC-CDMA system. *Arab. J. Sci. Eng.* **46**(2), 1465–1479 (2021)
20. N.H. Al-Ashwal, K.A. Al Soufy, F.S. Al-Kamali, M.A. Swillam, Performance evaluation of wireless compressed-image transmission over discrete Fourier transform-based orthogonal frequency division multiple access system. *J. Eng.* **2022**: 656–664 (2022) <https://doi.org/10.1049/tje2.12149>
21. R.L. Rivest, A. Shamir, L. Adleman, A method for obtaining digital signatures and public key crypto systems. *Commun. ACM.* **21**(2), 120–126 (1978)
22. Li. Li, Application of data image encryption technology in computer network information security. *Hindawi, Math. Probl. Eng.* **2022**, 8963756 (2022). <https://doi.org/10.1155/2022/8963756>
23. F.H. Mohammed Sediq Al-Kadei, H.A. Mardan, N.A. Minas, Speed up image encryption by using RSA algorithm. *6th International Conference on Advanced Computing & Communication Systems (ICACCS)* (2020)
24. A. Sahoo, P. Mohanty, P.C. Sethi, Image encryption using RSA algorithm, in *Intelligent Systems Lecture Notes in Networks and Systems 431*. ed. by S.K. Udgata et al. (Springer Nature Singapore Pte Ltd., Singapore, 2022). https://doi.org/10.1007/978-981-19-0901-6_5
25. M. Karolin, T. Meyyappan, Image encryption and decryption using RSA algorithm with share creation techniques. *Int. J. Eng. Adv. Technol. (IJEAT)* **9**(2) ISSN: 2249-8958 (2019)
26. E. Mehallal, D. Abed, A. Boukaache, A. Bouchemel, Enhancement of image transmission using chaotic interleaving with discrete wavelet transform-based single-carrier frequency division multiple access system. *Int. J. Commun. Syst. Commun. Syst.* **34**(7), e4728 (2021)
27. I. Eldokany, E.S.M. El-Rabaie, S.M. Elhalafawy, M.A. Zein Eldin, M.H. Shahieen, N.F. Soliman, M.A.M. El-Bendary, M.A. El-Naby, F.S. Al-kamali, I.F. Elashry, F.E. Abd El-Samie, Efficient transmission of encrypted images with OFDM in the presence of carrier frequency offset. *Wirel. Pers. Commun. Pers. Commun.* (2015). <https://doi.org/10.1007/s11277-015-2645-2>
28. S.A. Aliesawi, D.S. Alani, A.M. Awad, Secure image transmission over wireless network. *Int. J. Eng. Technol.* **7**(4), 2758–2764 (2018). <https://doi.org/10.14419/ijet.v7i4.15691>
29. K. Dharavathu, M. Satya Anu Radha, S. Sankar Naik, Image transmission and hiding through OFDM system with different encrypted schemes. *IJFRCSE*, ISSN: 2454-4248 (2015)
30. P. Hazowary, S. K. Dutta, R. Subadar, A comparison of image compression techniques over wireless fading channel. *Contemporary Issues in Communication, Cloud and Big Data Analytics* (Springer, Singapore, 2022), pp. 241–249
31. Z. Wang, Secure image transmission in wireless OFDM systems using secure block compression-encryption and symbol scrambling. *IEEE Access* (2019). <https://doi.org/10.1109/ACCESS.2019.2939266>
32. K. Dharavathu, S.A. Mosa, Efficient transmission of an encrypted image through a MIMO-OFDM system with different encryption schemes. *Sens. Imaging* **21**, 13 (2020). <https://doi.org/10.1007/s11220-020-0275-6>

Publisher's Note

Springer Nature remains neutral with regard to jurisdictional claims in published maps and institutional affiliations.